

# The magnetoelastic contribution to the steel internal damping

A. Lo Conte <sup>1</sup>

<sup>1</sup> Politecnico di Milano, Dipartimento di Meccanica, via Giuseppe La Masa 1, 20156 Milan, Italy.  
antonietta.loconte@polimi.it

**Abstract:** In this paper the steel internal damping due to both the thermoelastic and the magnetoelastic phenomenon has been investigated through a formulation based on thermodynamical potential joints with a hysteretic damping model. With the aim of focusing on the temperature transient in the solid, a first configuration has been considered, characterized by a steel rod with an imposed alternating pure shear strain in which only the thermoelastic contribution was studied. The magnetoelastic contribution was then introduced in a further configuration, in which a steel rod in free motion was subjected to torsion on its ends in presence of a constant magnetic field. A quantitative assessment of the influence of the magnetoelastic dissipation in steel has been computed according to the Sablik and Jiles model by giving a comparison between the thermoelastic and the prevailing magnetoelastic damping coefficient.

**Keywords:** Internal damping, magnetoelastic effect, thermodynamic formulation, thermoelastic damping

## 1. Introduction

Damping capability represents an important criterion for the selection of the materials for machines and components undergoing vibrations. The internal damping for metallic materials for engineering applications can be ascribed to different physical phenomena.

One of the main causes of the damping is the plastic strain, but this occurs only at stress levels greater than the usual design values. Another cause of the internal damping is given by the thermoelastic effect and by the diffusion of interstitial atoms that becomes important only beyond a critical frequency, that is over the frequency range involved in the vibration typically characterizing mechanical components.

The thermoelastic effect is the basis of thermography, a very common technique to analyze the stresses in components subjected to time-varying loads.

The temperature variations that occur in a homogeneous elastic solid are associated with the in-time variation of the stresses, and in the case of materials of common engineering interest such as steel and aluminum, they are generally of the order of  $0.1\text{ }^{\circ}\text{C} \div 0.01\text{ }^{\circ}\text{C}$ . Since these temperature values are related to the internal damping characteristics of the material, the heating rate measurement, together with the energy input, was used in the literature, as in [1], for the evaluation of the intrinsic material damping capacity. In particular, recent developments [2] and [3] show a particular interest in the evaluation of thermoelastic damping in micro beam resonators, as it is an important source of intrinsic energy dissipation and crucial to the design of the micro/nano devices.

The potential of the thermographic technique for the evaluation variation over time of the stress field in a component subjected to cyclic load includes both the ability to describe the physical phenomenon of the local dissipation of energy in the solid due to the thermoelastic effect, which through the Fourier equation allows to calculate the temporal variation of the temperature distribution, and a high degree of sensitivity in the measurement with infrared techniques of the temperature distribution in the area of interest.

**Citation:** Lastname, F.; Lastname, F.; Lastname, F. Title. *Materials* **2021**, *14*, x. <https://doi.org/10.3390/xxxxx>

Academic Editor: Firstname Lastname

Received: date

Accepted: date

Published: date

**Publisher's Note:** MDPI stays neutral with regard to jurisdictional claims in published maps and institutional affiliations.



**Copyright:** © 2021 by the authors. Submitted for possible open access publication under the terms and conditions of the Creative Commons Attribution (CC BY) license (<https://creativecommons.org/licenses/by/4.0/>).

The physical phenomenon of the local dissipation of mechanical energy into thermal energy can be defined through the definition of a constitutive law or based on a thermodynamic analysis of the mechanics of solids.

Finally, in a ferromagnetic materials, the magnetoelastic damping gives a significant contribution to the overall material damping, even at low stress levels and low frequency. The magnetoelastic aspect of damping has been previously analyzed in literature, as in [4] in which the damping capacity of highly magnetostrictive Fe-Ga solid-solution alloys was evaluated, or in [5], where dynamic stability of a soft ferromagnetic beam-plate in a transverse magnetic field was investigated, taking into account magnetoelastic interaction and magnetic damping. Moreover, in [6] measurements of the magneto-mechanical damping were evaluated in crystalline pure iron, nickel and cobalt bars, whereas in [7] it was analyzed for a cylindrical permalloy layer subjected to magnetic fields while performing free torsion oscillations. In recent developments, magneto-mechanical hysteresis damping behavior of Fe-Ga-La alloys has been studied in detail [8] and damping ratio based on magneto-thermoelasticity considerations was investigated [9] for Micro-Beam Resonators.

The magnetoelastic energy dissipation during a stress cycle can be interpreted in terms of two distinct magnetic phenomena: the magnetic hysteresis and the formation of local parasite currents [10]. A thorough physical interpretation of these phenomena can be found in literature, as in [11], [12], and [13], but the treatment of magnetoelastic dissipation from the quantitative point of view is still under investigation.

The treatment from the physical point of view is based on Weiss' model, considering that a ferromagnetic material is divided into magnetic subdomains, and that for the magnetic moment, deriving from natural magnetization, is close to saturation and is oriented along one of the most easily magnetizable directions of crystalline structure.

In the absence of external magnetic field, the magnetic moments of the single domain are casually oriented so that the total magnetic moment is zero or very low. After the application of a stress field, the followings occur:

1. a reversible rotation of the domain along the direction of the applied stress,
2. a reversible displacement of the contour of the domain,
3. a not reversible displacement of the contour of the domain.

The variation of the topology of magnetic domains due to the application of the stress field leads to a condition in which the vector resultant of the overall magnetic moment is still zero. However, a rotation of the magnetic moment of each domain occurs and a consequent magneto-strictive deformation that sums up to the purely mechanical deformation and, as a matter of fact, makes the material appear more deformable ( $\Delta E$  effect). The stress-strain curve, for low values of stress beyond which the phenomenon achieves saturation, has, indeed, a non-linear trend, and in case of time variable loads, it causes dissipation.

From the electromagnetic point of view, the reversible rotation of the domains and the reversible displacement of their contours give rise to a reversible rotation of the magnetic moment of the single domain. The not reversible displacement of domains' contour causes dissipative phenomena that, although due to the interaction among the magnetic moments, are generally described as caused by the friction among the contours of the magnetic domains themselves. In the presence of an externally applied constant magnetic field, the application of a time dependent stress due to the dissipative phenomena related to the magnetic interaction among domains gives rise to magnetic hysteresis. The application of a stress results, in a way, in being equivalent to the application of an equivalent (apparent) magnetic field [11]

In this work a thermodynamic formulation of the magnetoelastic phenomenon is coupled with a thermodynamic formulation of the thermoelastic one [14], [11]. The model allows to estimate the internal damping, both thermoelastic and magnetoelastic of steels and puts into evidence how, at low values of stress and frequency, the internal damping is mainly of a magnetoelastic nature.

## 2. Thermoelastic problem

As reported in [15], it is possible to express the thermodynamic potentials that concur to form the internal energy of the system (Free energy (A); Gibbs potential (G), enthalpy (H)) as functions of only three significant state variables, for example the temperature (T), the cubic strain ( $e_v$ ) and the conventional octahedral tangential component of the strain ( $\bar{e}$ ), and to obtain an expression of the Fourier equation for heat transfer capable of providing a quantitative evaluation of the associated thermoelastic effect and of the energetic phenomena:

$$\beta \nabla^2 T - \rho c_v \frac{\partial T}{\partial t} - \left[ \psi_1 \frac{\partial e_v}{\partial t} + \psi_2 \frac{\partial \bar{e}}{\partial t} \right] (T + T_0) = 0 \quad (1)$$

where the specific heat is:

$$c_v = c_v^*(T) + \frac{T + T_0}{\rho} \left[ 6\alpha \frac{dK}{dT} + 3\alpha \frac{d^2K}{dT^2} T \right] e_v - \frac{T + T_0}{\rho} \left[ \frac{1}{2} \frac{d^2K}{dT^2} e_v^2 + \frac{16}{3} \frac{d^2G}{dT^2} \bar{e}^2 \right] \quad (2)$$

$$\psi_1 = 3\alpha \frac{d(KT)}{dT} - \frac{dK}{dT} e_v \quad (3)$$

$$\psi_2 = \frac{32}{3} \frac{dG}{dT} \bar{e} \quad (4)$$

$$K = \frac{E}{3(1-2\nu)} \quad (5)$$

Strains are intended to be measured with respect to the reference configuration, which is characterized by the condition of zero stress and the base temperature  $T_0$  (i.e.  $T = 0$ ).

The thermodynamic analysis that leads to the Fourier equation for an isotropic elastic solid in the form of Equation (1) considers explicitly the dependence of the elastic modulus on temperature in the expression of the strain energy volumetric density [16]:

$$dL = \bar{\sigma} de_v + 4 \bar{\tau} d\bar{e} \quad (6)$$

where:

$\bar{\sigma}$  is the octahedral normal stress,

$\bar{\tau}$  is the octahedral tangential stress,

$e_v$  is the cubic strain,

$\bar{e}$  is the tangential octahedral strain.

The dependence of the elastic modulus of the material on temperature introduces a phase shift between the individual components of the strain tensor and the related components of the stress tensor, which results in the presence of coupling terms between the tensor field of the strains and the scalar field of temperatures. This means that, strictly speaking, the description of solids stressed with fatigue in an isothermal environment cannot be assigned to the equations of isothermal elasticity when considered separately from the heat equation, but rather requires the solution of the thermoelastic problem considered as a whole.

It can be observed that the approach based on thermodynamic potentials represents, in energetic terms, the phase shift between the components of the stress and strain tensor that, in the works of Zener [17] and [18] on internal damping, had instead been described through the introduction of a complex component of the elastic modulus. Equation (1) can also be compared with the equation proposed by Biot [19] for the solution of the thermoelastic problem:

$$\beta \nabla^2 T - \rho c_v \frac{\partial T}{\partial t} = 3 \alpha K (T + T_0) \frac{\partial e_v}{\partial t} \quad (7)$$

Biot's equation can be obtained from Eq. (1) considering the elastic modulus as not dependent on temperature and must be interpreted as an equation of limited validity, able to describe the problem only as a first approximation.

The variational formulation of the Biot thermoelasticity relations doesn't allow, in fact, to realistically include a class of basic problems of the solid mechanics, such as those characterized by zero values in the hydrostatic component of stress or deformation, or in any case small with respect to the values of the deviatoric component of stress or strain. If the equation proposed by Biot were unconditionally valid, in torsional stressed isotropic elastic solids there should be no thermoelastic effect and therefore the material stressed under these conditions would have zero internal damping.

### 3. Effect of stress on magnetic hysteresis

The application of a stress to a ferromagnetic material placed in a magnetic field, causes a variation in the intensity of magnetization that leads to its anhysteretic value [20]. As experimentally revealed, the factors that influence the variation of magnetization are the following:

- 1) how much the magnetization is lower or higher than its anhysteretic state,
- 2) how approaching to anhysteretic state is sensitive to the stress,
- 3) how the anhysteretic magnetization changes with stress.

In order to describe the effect of stress on the magnetic hysteresis the physical model of Jiles and Atherton [21], subsequently extended by Sablik and co-workers [22], [23] is considered for polycrystalline magnetic materials when subjected to uniaxial stress ( $\sigma$ ) aligned with the magnetic field. Both models refer to a condition in which the applied stress is constant, and the magnetic field is variable with time. The model proposed does not consider eddy currents effect, thermal viscosity, and demagnetization, but due to its relative simplicity and physical backgrounds is one of the most used ones.

In the anhysteretic state, that describes the thermodynamic equilibrium, a polycrystalline ferromagnetic element is considered a canonical ensemble of interacting magnetic moments. The effect of the interaction among the domains is represented as a contribution to the magnetic field, so that the effective magnetic field results as:

$$H_e = \bar{H} + \bar{\alpha} M_a + H_\sigma \quad (8)$$

where,  $\bar{H}$  is the applied magnetic field, the contribution  $\bar{\alpha} M_a$  is due to the magnetic interaction among the domains, while the contribution  $H_\sigma$  is due to the interaction among the domains, for the presence of the stress field.

The thermodynamic (or anhysteretic) expression for the magnetization  $M_a$  is obtained by means of the methods of statistical mechanics, considering the material as composed by pseudo-domains having defined contours. This hypothesis is compatible with the fact that the points of the anhysteretic curve correspond to thermodynamic equilibrium status, and every variation on that curve must be reversible, therefore it cannot involve variations of the contour of the domain. It is:

$$M_a = M_s \bar{L}(H_e/a) \quad (9)$$

in which the material constant ( $a$ ) is partially dependent on the microstructure. The contribution  $H_\sigma$  can be obtained considering that, in the case stress and magnetic field are co-axial, from thermodynamics we have:

$$\begin{aligned} G &= U - TS + (3/2)\sigma \lambda(M_a) \\ U &= (1/2)\bar{\alpha}\mu_0 M_a^2 \\ A &= G + \mu_0 \bar{H} M_a \end{aligned} \quad (10)$$

and the magnetoelastic energy is expressed as:

$$E_{\sigma} = \frac{3}{2} \sigma \lambda(M_a) \quad (11)$$

The effective magnetic field can be consequently written as:

$$H_e = \frac{1}{\mu_0} \left( \frac{\partial A}{\partial M_a} \right)_T = \bar{H} + \bar{\alpha} M_a + \frac{3}{2} \frac{\sigma}{\mu_0} \left( \frac{\partial \lambda(M_a)}{\partial M_a} \right)_T \quad (12)$$

from which the following can be obtained:

$$H_{\sigma} = \frac{3}{2} \frac{\sigma}{\mu_0} \left( \frac{\partial \lambda(M_a)}{\partial M_a} \right)_T \quad (13)$$

The irreversible contribution to magnetization deriving from the shift of the contours of the magnetic domains can be described as due to the presence of microstructural obstacles. The magnetic domains, during their displacement, engage with and disengage from such obstacles giving rise to a dissipative phenomenon (boundaries friction). The irreversible magnetization can be written as:

$$M_i = M_a - k \delta' \left( \frac{\partial M_i}{\partial B_e} \right) \quad (14)$$

where  $\delta' = +1$  or  $-1$ , when  $\bar{H}$  respectively increases or decreases and in which  $B_e = \mu_0 H_e$ .

In Equation (14) the second term, with the opposite sign with respect to  $\bar{H}$ , acts analogously to a mechanical friction term, giving rise to a dissipation. Equation (14) can be rewritten to obtain a differential equation whose solution delivers the irreversible magnetization:

$$\frac{\partial M_i}{\partial \bar{H}} = \frac{(M_a - M_i)}{\frac{\delta' k}{\mu_0} - \left( \bar{\alpha} + \frac{3\sigma}{2\mu_0} \left[ \frac{\partial^2 \lambda(M_a)}{\partial M_a^2} \right] \right)} (M_a - M_i) \quad (15)$$

From Equation (15) it results that the derivative of irreversible magnetization is a function of both the deviation of magnetization from its anhysteretic value ( $M_a - M_i$ ) and the factor ( $\delta' k$ ), that introduces the irreversibility and consequently the hysteresis. The given model includes a term that considers the bending of magnetic domains between two microstructural obstacles. Also, this term is a function of the deviation of magnetization from its anhysteretic value ( $M_a - M_i$ ) through a constant ( $c$ ) representing the ratio between initial magnetic susceptibility (not magnetized status) and the related anhysteretic value. Total magnetization can then be written as the sum of the irreversible magnetization and the last introduced contribution:

$$M = M_i + c(M_a - M_i) \quad (16)$$

Based on Equation (15) it can be remarked that the presence of a constant applied stress implies a variation of the slope of the hysteretic loop. Such variation is due to the contribution of the stress to the value of the effective magnetic field, and it is determined by magnetostriction  $\lambda(M_a)$ .

#### 4. Magnetic hysteresis of a cylindrical solid subjected to torsion

The Sablik-Jiles model, originally formulated for the case of coaxial stress and magnetic field, was subsequently extended to the case of a cylindrical solid undergoing constant torsion in presence of a magnetic field directed along the axis of the cylinder and time variable (Figure 1.a) [24].

From the physical point of view, the application of a couple in presence of a magnetic field  $\bar{H}$  causes a rotation ( $\theta$ ) of the magnetization vector  $M$  (Figure 1.b). In the case of a material such as steel, showing a positive derivative of the total magnetostriction with respect to magnetization, the magnetization vector rotates towards the direction along which the traction component acts, and it leaves the direction along which the compression component acts.

The magnetoelasticity energy is defined as the sum of the contributions due to the traction and the contribution due to compression, both not coaxial with the magnetic field. This can be written as:

$$E_{\sigma} = \frac{3}{2} \sigma [\lambda(M_a(\sigma))] (\cos^2 \theta - \nu \sin^2 \theta) + \frac{3}{2} (-\sigma) [\lambda(M_a(-\sigma))] (\sin^2 \theta - \nu \cos^2 \theta) \quad (17)$$

where  $\lambda(M_a(\sigma))$  is the magnetostriction due to the traction component ( $\sigma$ ) and  $\lambda(M_a(-\sigma))$  is the magnetostriction due to the compression component ( $-\sigma$ ).

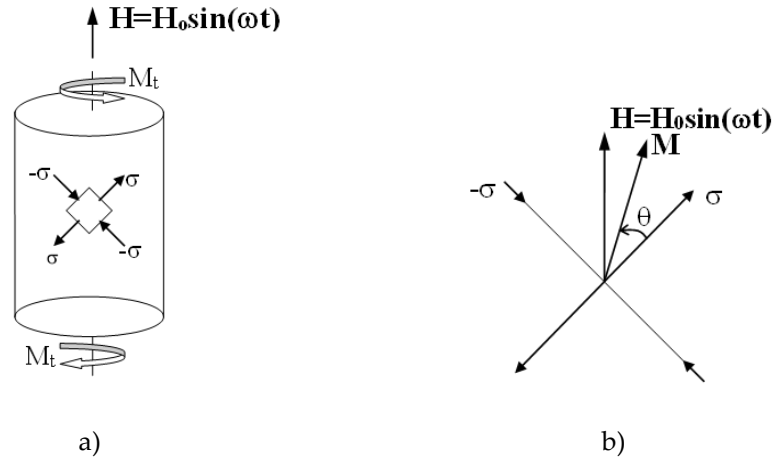


**Figure 1.** (a) Cylindrical solid subjected to torsion, principal stresses, and magnetic field oriented along the axis of the cylinder.; (b) Relative position of the magnetic vector  $\bar{H}$ , of the magnetization vector  $M$  and of the principal stresses due to the applied torsional moment.

Several formulations, both empirical and physical, have been proposed for the function  $\lambda(M_a)$ . The model under investigation derives the expression of the magnetostriction as a function of magnetization from the minimization of the internal energy with respect to the deformation and, in the case of a biaxial stress condition due to torsion, the magnetization is given by:

$$\frac{3}{2} \lambda(M_a(\sigma)) = \frac{|b|}{b} \left\{ \left[ \left( \frac{2b_s(\sigma)}{3Y} \right)^2 + \frac{2}{Y} (\Phi_{\text{mag}}(M_s) - \Phi_{\text{mag}}(M_a(\sigma))) \right]^{1/2} - \left[ \left( \frac{2b_s(\sigma)}{3Y} \right)^2 + \frac{2}{Y} \Phi_{\text{mag}}(M_s) \right]^{1/2} \right\} \quad (18)$$

where  $b$  is the isotropic magnetoelastic coupling constant and:

$$\Phi_{\text{mag}}(M_a(\sigma)) = \frac{1}{2} \mu_0 \alpha [M_a(\sigma)]^2 \quad (19)$$

$$b_{\vartheta}(\sigma) = b(1 + \nu) \left( 1 - \frac{1}{2} \sin^2 \vartheta \right)$$

$$b_{\vartheta}(-\sigma) = b(1 + \nu) \left( 1 - \frac{1}{2} \cos^2 \vartheta \right) \quad (20)$$

Since the trend of  $M_a(\sigma)$  with respect to  $\bar{H}$  is hysteretic, also the behavior of  $\lambda(M_a(\sigma))$  with respect to  $\bar{H}$  exhibits a hysteresis, but with a symmetric behavior across the  $\lambda$  axis. The effective magnetic field, acting along the direction of magnetization is then:

$$H_e = \bar{H} \cos(\pi/4 - \vartheta) + \bar{\alpha} M_a + H_{\sigma} \quad (21)$$

where:

$$H_{\sigma} = \frac{3}{2} \frac{\sigma}{\mu_0} \left[ \frac{\partial \lambda(M_a(\sigma))}{\partial M_a} (\cos^2 \theta - \nu \sin^2 \theta) - \frac{\partial \lambda(M_a(-\sigma))}{\partial M_a} (\sin^2 \theta - \nu \cos^2 \theta) \right] \quad (22)$$

Assuming, according to the definition of  $\lambda(M_a(\sigma))$  and  $\lambda(M_a(-\sigma))$ :

$$\begin{aligned} \frac{\partial \lambda(M_a(\sigma))}{\partial M_a} &\rightarrow \frac{\partial \lambda(M_a(\sigma))}{\partial M_a(\sigma)} \\ \frac{\partial \lambda(M_a(-\sigma))}{\partial M_a} &\rightarrow \frac{\partial \lambda(M_a(-\sigma))}{\partial M_a(-\sigma)} \end{aligned} \quad (23)$$

in the considered case the component of the magnetization acting along the direction of application of the magnetic field is given by:

$$M_z = M \cos\left(\frac{\pi}{4} - \vartheta\right) \quad (24)$$

and Equation (15) becomes:

$$\frac{\partial M_i}{\partial \bar{H}} = \frac{(M_a - M_i) \cos(\pi/4 - \vartheta)}{\frac{\delta' k}{\mu_0} - \left( \bar{\alpha} + \frac{3\sigma}{2\mu_0} [\Lambda(\sigma)] \right) (M_a - M_i)} \quad (25)$$

where:

$$\Lambda(\sigma) = \frac{\partial^2 \lambda(M_a(\sigma))}{\partial M_a(\sigma)^2} (\cos^2 \theta - \nu \sin^2 \vartheta) - \frac{\partial^2 \lambda(M_a(-\sigma))}{\partial M_a(-\sigma)^2} (\sin^2 \theta - \nu \cos^2 \vartheta) \quad (26)$$

To get the angle of rotation of the magnetization with respect to the direction of the applied magnetic field, when the cylindrical solid is subjected to torsion, the potential energy is considered:

$$\Omega = -\mu_0 \bar{H} M_a \cos(\pi/4 - \vartheta) - E_{\sigma} \quad (27)$$

The condition  $d\Omega/d\vartheta = 0$  delivers the value of  $\vartheta$  for the configuration of equilibrium corresponding to the magnetic field and to the applied torsional moment. The following is obtained:

$$\vartheta = \frac{1}{2} \sin^{-1} \left\{ \frac{-1 + \sqrt{1 + 4A'}}{2A'} \right\} \quad (28)$$

where:

$$A' = 8 \left\{ \frac{3\sigma(1+\nu)}{2\mu_0 \bar{H} M_a} \left( \bar{\lambda}_a(\sigma, -\sigma) \right) \right\}^2 \quad (29)$$

$$\bar{\lambda}_a(\sigma, -\sigma) = \frac{1}{2} [\lambda(M_a(\sigma)) + \lambda(M_a(-\sigma))] \quad (30)$$

The initial value ( $\vartheta_0$ ) of the angle  $\vartheta$  is a function of the initial anhysteretic magnetization. Subsequently, for increasing torsion torque,  $\vartheta$  decreases with respect to its initial value.

## 5. Torsional pendulum with hysteretic damping model

The calculation of the internal damping is carried out for a configuration in which a circular cylindrical solid is inserted in a torsional pendulum device for the measurement of the internal damping and subjected to a constant magnetic field equal to the earth magnetic field and acting along the axis of the cylindrical solid.

The torsional pendulum is a measurement technique that exploits the free vibration of the system made by the solid under testing that corresponds to the torsional stiffness of the system, and a disk corresponding to the torsional moment of inertia of the system. The configuration is reported in Figure 2.

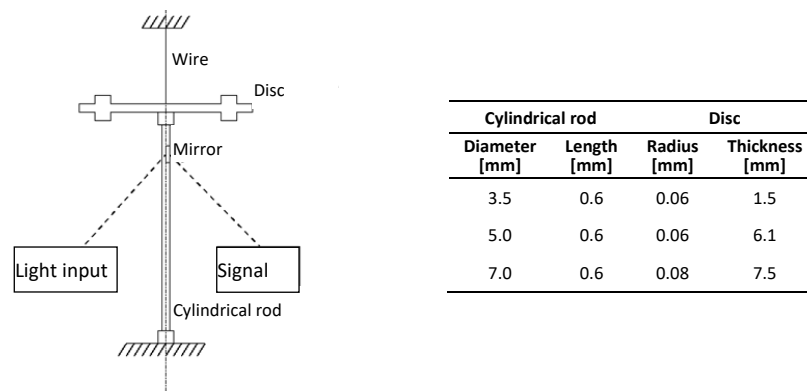


Figure 2. Torsional pendulum for damping measurement (dimensions for  $f=15$  Hz).

The internal damping ( $\eta$ ), related to a given  $n$ -th cycle of oscillation, evaluated from the evolution of the angular oscillation of the disk, can be expressed as a function of logarithmic decrement, as the ratio between two consecutive peaks of the  $n$ -th and  $n$ -th+1 cycles:

$$\delta_n = \ln \frac{A_n}{A_{n+1}} \quad (31)$$

where  $A_n$  represents the amplitude of the  $n$ -th peak and  $A_{n+1}$  represents the amplitude of the subsequent peak of the oscillation.

The introduction of a dissipative term in Eq (1) allows to apply the equation to the calculation of the temperature distribution, and therefore of the internal damping, of the cylindrical solid with circular cross section that represents the test sample inserted in a torsional pendulum.

As shown by experimental evidence [25], the internal damping is mainly due to the relaxation phenomenon, strongly dependent on temperature and frequency, and to mechanical hysteresis, which demonstrates a strong dependence on the amplitude and does not show a significant dependence on the frequency.

In the present work temperature values for which relaxation is an unimportant phenomenon are taken into account and the dissipative term to be introduced in Eq. (1) is expressed on the basis of a hysteretic model [26].

This model describes the internal damping as a phenomenon due to irreversible transformations in the elastic solid subjected to cyclic deformations. Furthermore, it provides that the area between the stress-strain curve in the loading phase and the one in the unloading phase is proportional to the dissipated energy and doesn't depend on the frequency at which the load cycle is covered but depends on the amplitude. The hypotheses of frequency independence and amplitude dependence find physical confirmation respectively in the fact that the stress-strain laws can be assumed to be independent of time and in the fact that, since hysteresis is a non-linear phenomenon, the dissipation of energy per cycle must necessarily increase as the amplitude of the deformation increases.

Given  $\bar{\varphi} = \varphi_r + i\varphi_i$  the angle of rotation of the pendulum and  $\bar{K}_\varphi$  its torsional stiffness, the torsional torque is written as:

$$M_t = \bar{K}_\varphi \times \bar{\varphi} = K_\varphi (1 + i\chi) \varphi \quad (32)$$

where the axis  $\varphi$  is assumed as real axis, the parameter  $\chi$  is the hysteretic damping factor with the condition  $\chi \ll 1$ .

The torsional torque  $M_t$  is then given by the composition of a component in-phase with the angle of rotation ( $K_\varphi \cdot \varphi$ ) and of a component  $90^\circ$  out-of-phase ( $\chi \cdot K_\varphi \cdot \varphi$ ) that gives rise to a mechanical energy dissipation into thermal energy for a cycle that can be expressed as the sum of a thermoelastic and a magnetoelastic contribution:

$$\Delta W = (\chi \cdot K_\varphi \varphi_0^2 \pi)_{\text{thermoelastic}} + \Delta W_{\text{magnetoelastic}} \quad (33)$$

The dissipated energy  $\Delta W$  corresponds to the area of the hysteresis cycle which, for the assumed damping model, is elliptical with a major axis equal to  $\varphi_0$  and a minor axis equal to  $\chi \cdot K_\varphi \cdot \varphi_0$ .

### 6. Thermoelastic solution for a rod subjected to alternating pure shear strain

With the aim of analyzing the trend of the temperature transient, the configuration of a steel rod with an imposed alternating pure shear strain was initially analyzed, in which only the thermoelastic contribution was studied.

The associated principal strains of a pure shear strain ( $\gamma$ ) are:

$$\begin{aligned} e_1 &= \gamma \frac{r}{2R} \sin(2\pi ft) + \alpha T \\ e_2 &= \alpha T \\ e_3 &= -\gamma \frac{r}{2R} \sin(2\pi ft) + \alpha T \end{aligned} \tag{3}$$

where  $f$  indicates the frequency of the imposed strain cycle. In such conditions the following is obtained:

$$\bar{e} = \sqrt{\frac{2}{3}} \gamma \frac{r}{R} \sin(2\pi f t) \tag{35}$$

$$e_v = 3\alpha T \tag{36}$$

The presence of imposed strains allows to focus attention on the temperature variation of the cylindrical solid. Eq. (1) can consequently be expressed as:

$$\beta \nabla^2 T - \left[ \rho c_v + (T + T_0) \psi_1 \left( 3T \frac{d\alpha}{dT} + 3\alpha \right) \right] \frac{\partial T}{\partial t} - \psi_2 (T + T_0) \left( \sqrt{\frac{2}{3}} \gamma \frac{r}{R} 2\pi f \sin(2\pi f t) \right) = 0 \tag{37}$$

with the following boundary conditions:

$$\begin{aligned} \text{for } t=0 & \quad T=0 \\ \text{for } r=0 & \quad \frac{\partial T}{\partial r} = 0 \\ \text{for } r=R & \quad \frac{\partial T}{\partial r} + h_t T = 0 \end{aligned}$$

where  $h_t$  is the heat exchange coefficient.

The solution of the problem can be carried out analytically or numerically. In the following a numerical solution was applied to the case of a cylindrical solid, with a diameter of 3.5 mm, 7 mm, and 14 mm in 2¼Cr-1Mo steel whose mechanical and thermal characteristics as a function of temperature, for a range between 25 °C and 300 °C, are reported in Table 1.

**Table 1.** Dependence on temperature of elastic and thermal parameters [16].

$E$	$(215 - 0.085 T) \cdot 10^9$	N/mm <sup>2</sup>
$\bar{G}$	$(85 - 0.036 T) \cdot 10^9$	N/mm <sup>2</sup>
$c_v$	$(425 + 0.416 T)$	J/(kg °C)
$\alpha$	$(11.3 - 0.014 T - 1 \cdot 10^{-5} T^2) \cdot 10^{-6}$	1/°C
$\beta$	$(35.75 - 0.0223 T - 1 \cdot 10^{-4} T^2)$	W/(m °C)
$h_t$	10	W/(m <sup>2</sup> °C)

The equation for the computation of the temperature distribution in the cylindrical solid subjected to torsion was solved by means of a finite difference numerical method.

numerical solution considers the temperature of the solid as a function of the radial coordinate  $r$ , and takes into account the dependence on the temperature of the elastic constants of the material and of the quantities that govern the heat exchange. Once the temperature distribution is known, the local entropy density along the radial coordinate  $r$  is then calculated from the following equation:

$$P(q)=(T+T_0)P(s)=\beta\frac{(\text{grad}T)^2}{T+T_0} \quad (38)$$

The material internal damping is expressed through the damping coefficient  $\eta$ :

$$\eta=\frac{\Delta W}{\Xi}=2\delta \quad (39)$$

where:

$\Delta W$  is the mechanical energy dissipated in heat in a period,

$\Xi$  is the amplitude of the function describing the elastic energy stored in the volume material into which the dissipation takes place,

$\delta$  is the logarithmic decrement (Eq. 31).

At local scale, indicating with  $t^*$  the period of the oscillation, the following holds:

$$W=\int_0^{t^*} P(q)\cdot dt \quad (40)$$

From Eq. (39) it is possible to calculate the local damping coefficient through a simple time integration.

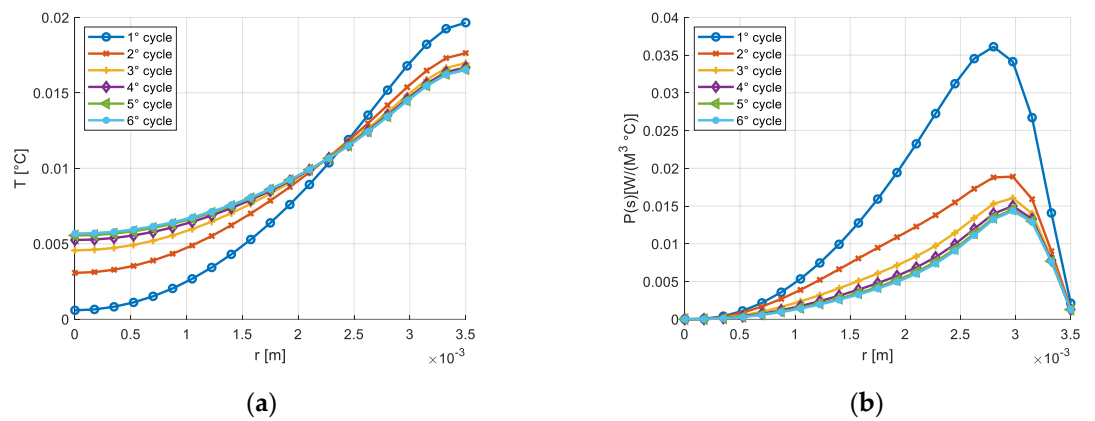
The results relating to cycle with imposed strain are shown below, the amplitude of which is defined by a maximum value of the pure shear strain on the contour of the circular section  $\gamma_{\max} = 1200 \cdot 10^{-6}$ . Once the strain cycle was fixed, two different values of the frequency of the strain cycle, equal to 15 Hz and 150 Hz, were examined and the absolute temperature of the solid equal to 300 K was assumed.

Figure 3 shows the temperature transient and the entropy production on the section of the cylindrical solid considering the frequency of 15 Hz. The trend, represented for different number of cycles, is deeply influenced by the heat exchange at the external surface, whose temperature remains constant and equal to 300 K. The temperature transients and the volumetric density of the entropy production in the node placed on the axis of the rod, and in the node placed at a distance from the axis equal to  $R/2$  are reported respectively in Figure 4 and Figure 5. A similar thermal transient is observed, but the entropy production on the axis of the rod is negligible.

The values of the local internal damping as function of the radial coordinate, obtained production of the cycle, are shown in Table 2.

The temperature transient and the entropy production on the section of the cylindrical solid considering the frequency of 15 Hz are reported in Figure 6. Moving from 15 Hz to 150 Hz, a faster thermal transient on the section with higher temperature values, can be observed.

With the aim of analyzing the influence of the strain cycle amplitude on the results, the frequency was fixed at 15 Hz, a second value of the imposed strain cycle amplitude ( $\gamma_{\max} = 600 \mu\gamma$ ) was considered in addition to the value considered previously ( $\gamma_{\max} = 1200 \mu\gamma$ ). The trend of the temperature and of the volumetric density of the entropy production on the cylinder section are shown in Figure 7, in which it is possible to observe the significant decrease of both maximum temperature variation and of the entropy production as the amplitude of the strain cycle decreases with cycles.



**Figure 3.** (a) Temperature variation on the section of the cylindrical solid,  $\gamma_{\max} = 1200 \mu\gamma$ ,  $f = 15$  Hz; (b) Entropy production on the section of the cylindrical solid,  $\gamma_{\max} = 1200 \mu\gamma$ ,  $f = 15$  Hz.

367  
368

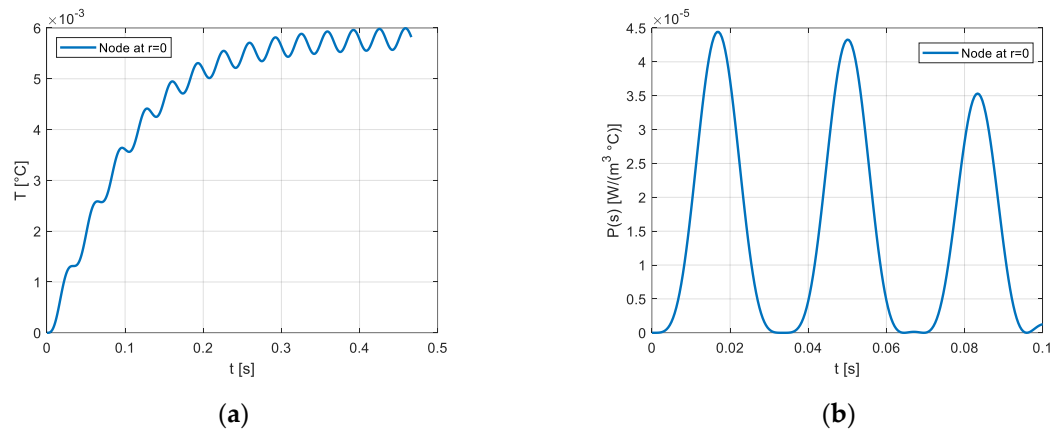


**Figure 4.** (a) Temperature transient in the central node,  $\gamma_{\max} = 1200 \mu\gamma$ ,  $f = 15$  Hz; (b) Transient of the Entropy production on the node adjacent to the central node  $\gamma_{\max} = 1200 \mu\gamma$ ,  $f = 15$  Hz.

369  
370

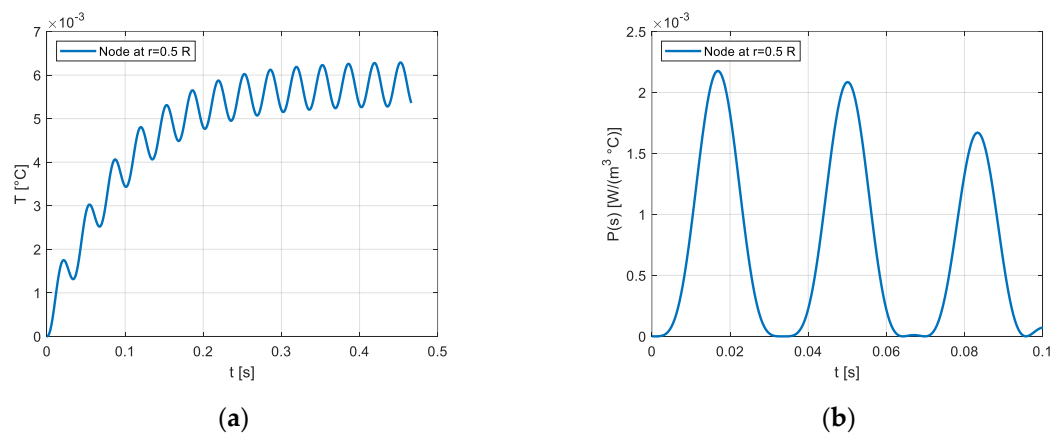


**Figure 5.** (a) Temperature transient on the node located at 0.5 R  $\gamma_{\max} = 1200 \mu\gamma$ ,  $f = 15$  Hz; (b) Transient of entropy production on the node located at 0.5 R  $\gamma_{\max} = 1200 \mu\gamma$ ,  $f = 15$  Hz.

371  
372

**Table 2.** Local damping coefficients as a function of radial coordinate, values are expressed in  $10^{-4}$

373

Node location	0.1 R	0.2 R	0.3 R	0.4 R	0.5 R	0.6 R	0.7 R	0.8 R	0.9 R
Damping $\eta$	0.38	1.06	1.21	1.30	1.32	1.34	1.44	1.66	1.67

374

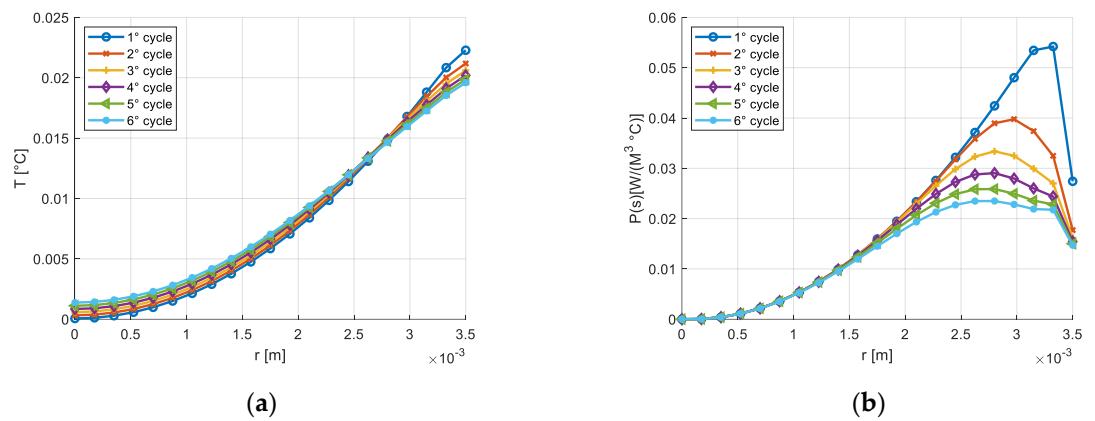


Figure 6. (a) Temperature variation on the section of the cylindrical solid,  $\gamma_{max} = 1200 \mu\gamma$ ,  $f = 150$  Hz; (b) Entropy production on the section of the cylindrical solid  $\gamma_{max} = 1200 \mu\gamma$ ,  $f = 150$  Hz.

375  
376

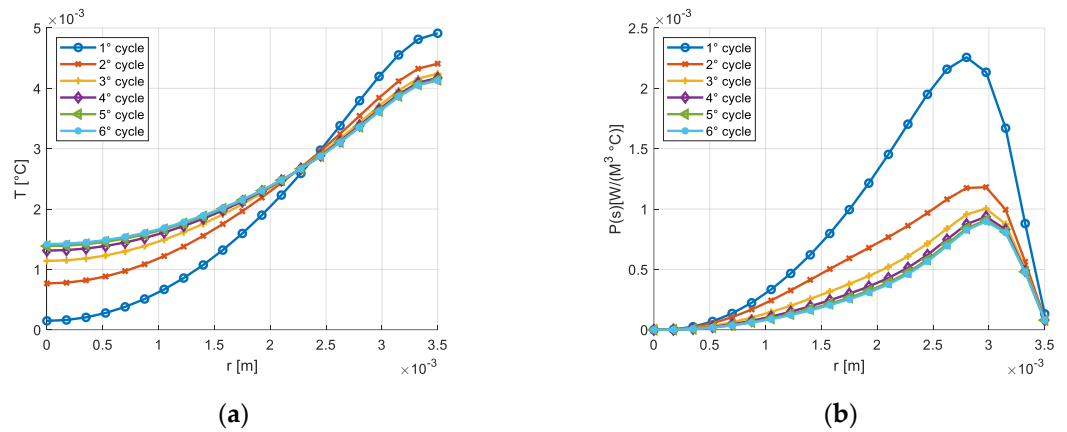


Figure 7. (a) Temperature variation on the section of the cylindrical solid,  $\gamma_{max} = 600 \mu\gamma$ ,  $f = 15$  Hz; (b) Entropy production on the section of the cylindrical solid  $\gamma_{max} = 600 \mu\gamma$ ,  $f = 15$  Hz.

377  
378

A numerical experimentation was also conducted for the calculation of the overall damping of the cylinder considering its diameter as variable, to evaluate the influence of the dimensions of the specimen on the results obtained. The overall damping values for a cylinder with diameters of 14 mm and 3.5 mm are shown in the following table and compared with the results obtained for the diameter of 7 mm previously analyzed.

379  
380  
381  
382  
383

Table 3. Overall damping coefficients as a function of the diameter, values are expressed in  $10^{-4}$

384

Diameter (mm)	3.5	7	14
Damping $\eta$	3.0	1.3	0.1

385

### 7. Solution for a rod subjected to torsion in free motion

386

With the aim of analyzing the dissipated energy of a thermoelastic nature and, of a magnetoelastic nature, for the evaluation of the damping in the oscillation cycles, the condition of free motion was considered, with the hypothesis of hysteretic damping.

387  
388  
389

The equation of free motion of the torsional pendulum, with the hypothesis of hysteretic damping described by the hysteretic damping factor ( $\chi$ ), is written as:

390  
391

$$M_\phi \ddot{\phi} + K_\phi (1 + i\chi) \phi = 0 \tag{40}$$

The solution presented in [27], for the calculation of the only component of thermoelastic damping, is herein reported and can be expressed as:

392  
393

$$\varphi = \varphi_0 \exp \left\{ -\omega t \left[ \frac{\sqrt{(1+\chi^2)}-1}{2} \right]^{1/2} \right\} \cdot \cos \left\{ \omega t \left[ \frac{\sqrt{(1+\chi^2)}+1}{2} \right]^{1/2} + \phi \right\} \quad (41)$$

where  $\varphi_0$  and  $\phi$  are two constants to be determined based on the initial conditions, and the logarithmic decrement is given by:

$$\delta = \frac{2 \pi \chi}{1 + \sqrt{(1+\chi^2)}} \cong 2\pi\chi \quad (42)$$

having assumed  $\chi \ll 1$ .

Considering Equation (41) and assuming as unit rate the term  $\left( \frac{\sqrt{(1+\chi^2)}+1}{2} \right)^{1/2}$ , according to the hypothesis  $\chi \ll 1$  the strains tangential octahedral component can be expressed as:

$$\bar{e} = \sqrt{\frac{2}{3}} \frac{r}{2} \varphi_0 \exp \left\{ -\omega t \left[ \frac{\sqrt{(1+\chi^2)}-1}{2} \right]^{1/2} \right\} \cdot \cos\{\omega t + \phi\} \quad (43)$$

Where  $r$  represents the radial coordinate of the circular cross section of the cylinder.

Cubic strain, due solely to the effect of thermal expansion, is instead written as:

$$e_v = 3\alpha T \quad (44)$$

Fourier's equation for the cylindrical solid with circular section that oscillates in free motion with a model of hysteretic damping results in:

$$\begin{aligned} & \beta \nabla^2 T - \left[ \rho c_v + (T+T_0) \psi_1 \left( 3T \frac{d\alpha}{dT} + 3\alpha \right) \right] \frac{\partial T}{\partial t} + \\ & - \psi_2 (T+T_0) \left( \sqrt{\frac{2}{3}} \frac{r}{2} \varphi_0 \omega \exp\{-h\omega t\} \left[ \left( -\frac{dh}{dt} t - h \right) \cos\{\omega t + \phi\} - \sin\{\omega t + \phi\} \right] \right) = 0 \end{aligned} \quad (45)$$

where the damping ratio ( $h$ ) is expressed as:

$$h = \left[ \frac{\sqrt{(1+\chi^2)}-1}{2} \right]^{1/2} \quad (46)$$

while the boundary conditions are the following:

$$\begin{array}{lll} \text{for} & t=0 & T=0 \\ \text{for} & r=0 & \frac{\partial T}{\partial r} = 0 \\ \text{for} & r=R & \frac{\partial T}{\partial r} + h_t T = 0 \end{array}$$

Where  $h_t$  is the thermal exchange coefficient and  $R$  is the radius of the circular section of the cylinder. Equation (45) is solved numerically at finite differences considering the temperature function of the radial coordinate only and considering the dependence of the elastic constant on temperature and on the constants that regulate the thermal exchange.

The calculus of the contribution  $\Delta W_{\text{magnetoelastic}}$  in Equation (33) has been carried out according to the model presented in Section 4, but considering the intensity of the magnetic field oriented along the axis of the cylinder as variable, in accordance with the amplitude of  $\theta$ , and with the corresponding torque moment.

From the numerical point of view, the procedure is as follows. Assuming the initial magnetic field is known, the relative value of the anhysteretic magnetization ( $M_a$ ) and the initial value of the angle  $\theta$  is calculated. Subsequently, at each time step of Equation (45):

1. the effective magnetic field ( $H_e$ ) and the variation  $d\bar{H}$  due to the increment of the applied torque are calculated, from the knowledge of the value of  $\theta$ , of the previous value of  $M_a$  and of the derivatives  $\partial \lambda / \partial M_a(\sigma)$  and  $\partial \lambda / \partial M_a(-\sigma)$ ;
2. a new value of  $M_a$  can be calculated;

3. the variation  $dM_i$  can be calculated from  $\theta$  and  $d\bar{H}$  from the previous values of  $M_a$  and  $M_i$ ; 420  
421
4. a new value of  $M_i$  is computed from  $dM_i$  and from the previous  $M_i$ ; 422
5.  $M$  and the related component  $M_z$  are then calculated. 423

Steps 1) to 5) are processed until a complete oscillation cycle of  $M_t$ , corresponding to the 424  
completion of a cycle of magnetic hysteresis, from which  $\Delta W_{\text{magnetoelastic}}$  can be evaluated. 425

The dissipated energy, of thermoelastic and magnetoelastic nature, enables to calcu- 426  
late the damping of the cycle of oscillation applied to the subsequent cycle of the pendu- 427  
lum. 428

The results of a circular cylindrical solid with 5 mm diameter, made of steel 2¼Cr1Mo 429  
are presented. The natural frequency of the system is 15 Hz, the amplitude of the initial 430  
shear strain is assumed to be equal to 800  $\mu\gamma$ , 1000  $\mu\gamma$  e 1200  $\mu\gamma$ , and the temperature is 431  
27°C. 432

The mechanical and thermal parameters of the considered material are reported in 433  
Table 1, considering their dependence on the temperature. The magnetic parameters are 434  
reported in Table 4. 435

Looking at Figure 8, for the first oscillation cycle starting from 1200  $\mu\gamma$ , it can be ob- 436  
served that, depending on the applied torque, the angle  $\theta$  the axis of magnetization of the 437  
solid varies between 30° and 57°. The former corresponds to the maximum torque, in 438  
which the principal stresses assume the sign reported in Figure 1a), the latter corresponds 439  
to the first inversion of the torque. 440

In accordance with the model herein proposed, since in Equation (39) both  $P(s)$  and 441  
 $\Xi$  have a different distribution depending on the geometry of the system and on the dis- 442  
tribution of stress (or strain), a local damping coefficient and a global damping coefficient 443  
of the entire system can be considered for the system in a specific configuration. 444

The comparison between the damping thermoelastic coefficient and the magneto- 445  
elastic coefficient as a function of radial coordinate is reported in Figure 9, for the stable 446  
cycle corresponding to an initial maximum shear strain of 1200  $\mu\gamma$ . It can be remarked 447  
that the magnetoelastic local damping shows a limited variability with radial coordinate, 448  
and that it is prevailing with respect to the thermoelastic damping. The overall damping 449  
of the system is reported in Table 5 for the three different values of initial maximum strain. 450  
It is worth remarking that the overall damping can't be described in a general way the 451  
damping independently from the examined configuration. 452

The obtained results confirm that the internal damping is mainly of magnetoelastic 453  
nature. Both contributions to damping increase with the amplitude. 454

Table 4. Magnetic parameters [23]. 455

$\bar{H}$	36	Asp/m
$M_s$	1.585 e+06	Asp/m
$\lambda_s$	2.07 e-05	
$c$	0.15	
$a$	2350	Asp/m
$\bar{\alpha}$	7.09 e-05	W/(m °C)]
$k/\mu_0$	2400	Asp/m
$\mu_0$	12.57 e-07	H/m
$b$	-0.242 e+07	N/m <sup>2</sup>

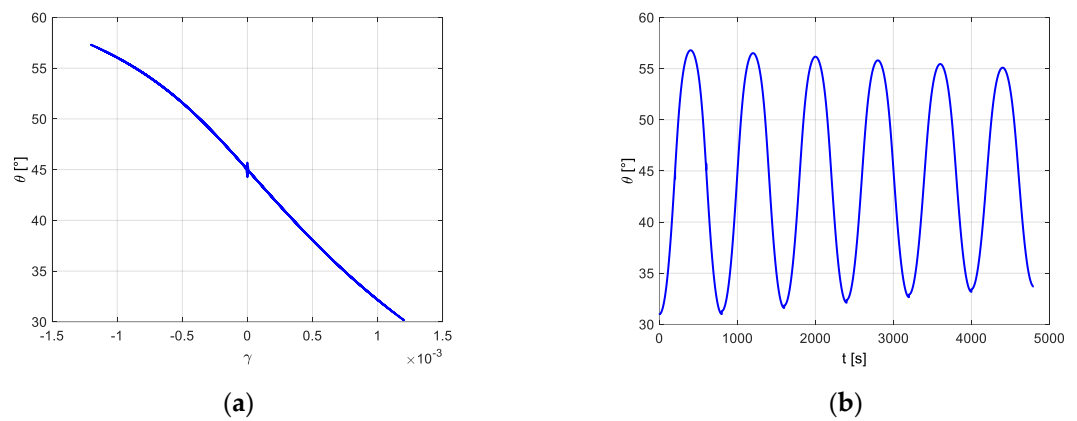


**Figure 8.** a) Rotation of the magnetization with respect to the maximum strain, in the first oscillation cycle. b) Rotation of the magnetization vs time, in the first six cycles.

457  
458

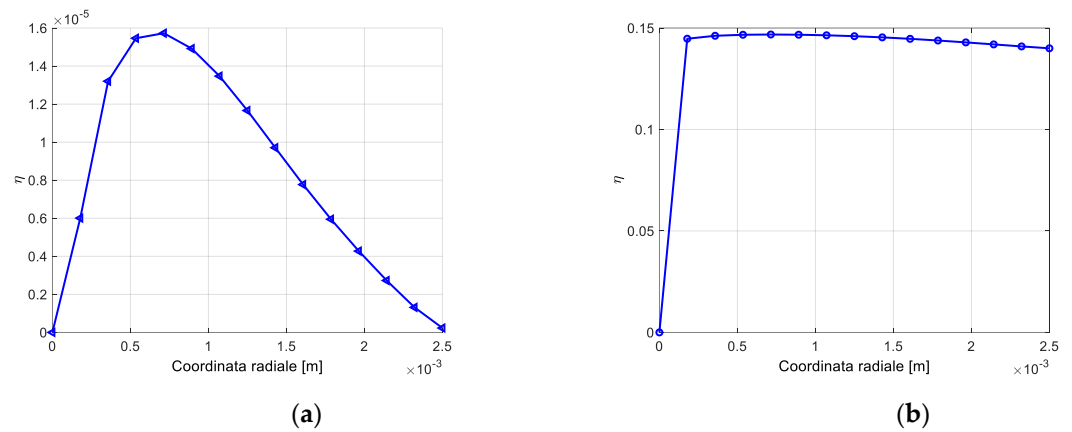


**Figure 9.** a) Local thermoelastic damping coefficient  $\eta$  as a function of radial coordinate, stable cycle. b) Local magnetoelastic damping coefficient as a function of radial coordinate, stable cycle.

459  
460  
461

**Table 5.** Internal thermoelastic and magnetoelastic damping coefficients varying the maximum strain amplitude. Values refer to the stabilized cycle.

462  
463

	800 $\mu\gamma$	1000 $\mu\gamma$	1200 $\mu\gamma$
Thermoelastic damping coefficient $\eta$	$4 \cdot 10^{-4}$	$6 \cdot 10^{-4}$	$9 \cdot 10^{-4}$
Magnetoelastic damping coefficient $\eta$	$12 \cdot 10^{-2}$	$12.7 \cdot 10^{-2}$	$13.1 \cdot 10^{-2}$

464

### 9. Conclusions

465

In the present work the internal damping due to both thermoelastic and magnetoelastic effects was calculated for a cylindrical solid subjected to torque and inserted into a constant magnetic field.

466  
467  
468

To analyze the trend of the temperature variation in the solid, it was reputed more appropriate to firstly consider an alternating torsion configuration with imposed sliding rather than the free motion of the solid itself, by evaluating exclusively the thermoelastic effect. The results obtained show how the variation of the imposed cycle frequency affected the temperature field on the section of the solid, as an increase in frequency led to a similar trend of the temperature transient for higher temperature values. Also worthy of mention is the decrease in the maximum temperature variation of the specimen and in the production of entropy with the decrease in the amplitude of the deformation cycle.

469  
470  
471  
472  
473  
474  
475  
476

It should be noted that the proposed solution, based on thermodynamic analysis and on a model of hysteretic damping, is of more general validity than that which would have been obtained with the Biot equation.

This solution therefore shows how the internal damping of the material should not be interpreted as a mechanical characteristic, but rather as the result of thermodynamic phenomena strongly dependent on the boundary conditions of the system.

In fact, the numerical calculations based on the proposed solution allow to obtain an evaluation of the energy dissipated by the irreversible processes, even in the case in question of a solid stressed with alternating torsion, for which the Biot solution would provide a null estimate of the thermal effect.

Given the great importance of the magnetoelastic contribution to damping in materials such as steel, it was however necessary to consider a configuration in which the solid was subjected to torsion in free motion. The magnetoelastic contribution to damping was evaluated adopting the model of Sablik-Jiles, that proved to be valid for the description of the magnetoelastic internal damping in a cylindrical solid subjected to torsion, in presence of a constant magnetic field directed along the axis of the cylinder. The results of the comparison between the damping thermoelastic coefficient and the magnetoelastic coefficient show that the latter is characterized by a limited variability with radial coordinate and that, as expected, it is prevailing with respect to the thermoelastic damping. These outcomes confirmed that the internal steel damping is mainly linked to the magnetoelastic effect, making the in-depth treatment of the magneto-mechanical damping from a quantitative point of view extremely relevant.

**Conflicts of Interest:** “The authors declare no conflict of interest.”

#### List of symbols

$A$	Free energy;
$E$	Young modulus;
$E_{\sigma}$	Magnetoelastic energy;
$G$	Gibbs free energy;
$\bar{G}$	Tangential elasticity modulus;
$H$	Enthalpy;
$\bar{H}$	Applied magnetic field;
$H_e$	Effective magnetic field;
$H_{\sigma}$	Contribution to magnetic field due to the magnetoelastic domains interaction;
$K$	Bulk modulus
$\bar{K}_{\varphi}$	Stiffness of the torsional pendulum;
$L$	Mechanical energy;
$\bar{L}$	Langevin's function;
$M$	Total magnetisation;
$M_a$	Anhysteretic magnetisation;
$M_i$	Irreversible magnetisation ;
$M_t$	Torque;
$M_s$	Saturation magnetization value;

$M_z$	Component of the total magnetization along the direction of the magnetic field;
$S$	Entropy;
$R$	Radius of the rod circular cross section;
$T$	Absolute temperature in the solid measured with respect to base temperature;
$T_0$	Base temperature of the solid;
$U$	Internal energy;
$\Delta W$	Mechanical energy dissipated in a cycle;
$a$	Energy of magnetoelastic coupling;
$b$	Isotropic magnetoelastic coupling constant;
$c$	Ratio between the susceptibility in the demagnetised status and the related anhysteretic value;
$c_v$	Specific heat;
$c_v^*$	Specific heat at the temperature ( $T$ ) and zero strain;
$e_v$	Cubic strain;
$\bar{e}$	Octahedral component of strain;
$h$	Damping ratio;
$k$	Constant of the material depending on the density of microstructural obstacles;
$t$	Time;
$\Xi$	Amplitude of the function describing the cumulated elastic energy in the volume in which the dissipation $\Delta W$ takes place;
$\Omega$	Potential energy
$\bar{\alpha}$	Parameter of magnetic interaction among domains;
$\alpha$	Linear dilatation coefficient;
$\beta$	Thermal conductivity;
$\chi$	Hysteretic damping factor;
$\delta$	Logarithm decrement;
$\delta'$	Parameter for the introduction of magnetic hysteresis;
$\bar{\varphi}$	Rotation angle of the torsional pendulum;
$\gamma$	Shear strain;
$\eta$	Damping coefficient;
$\lambda$	Magnetostriction;
$\mu_0$	Magnetic permeability in vacuum;
$\rho$	Density;
$\sigma$	Stress;
$\bar{\sigma}$	Octahedral normal stress;

$\theta$	Rotation of the magnetization with respect to the direction of the applied magnetic field;
$\bar{\tau}$	Octahedral shear stress
$\nu$	Poisson's coefficient.
$\chi$	Hysteretic damping factor;

## References

- J. Åberg, B. Widell, «Measurement of intrinsic material damping using differential calorimetry on specimens under uniaxial tension,» *Thermochimica Acta* 411, pp. 125-131, August 2003. 502
- Bingdong Gu, T. He, «Thermoelastic damping analysis in micro-beam resonators considering nonlocal strain gradient based on dual-phase-lag model,» *International Journal of Heat and Mass Transfer*, vol. 180, 121771, 2021. 505
- H. Zhou, H. Jiang «Thermoelastic damping in the size-dependent micro/nanobeam resonator,» *Thin-Walled Structures*, vol. 169, 108437, 2021. 507
- M. Ishimoto, H. Numakura, «Magnetoelastic damping in Fe–Ga solid-solution alloys,» *Materials Science and Engineering* 442, p. 195–198, 2006 509
- Xingzhe Wang, J.S. Lee «Dynamic Stability of Ferromagnetic Beam-Plates with Magnetoelastic Interaction and Magnetic Damping in Transverse Magnetic Fields,» *Journal of Engineering Mechanics*, 132(4), pp. 422-428, April 2006. 511
- A.L. Morales, A.J.Nieto, «Field dependent elastic modulus and damping in pure iron, nickel and cobalt,» *Journal of Magnetism and Magnetic Materials* 322, pp. 1952-1961, January 2010. 513
- A Ercuta, I. Mihalca «Magnetomechanical damping and magnetoelastic hysteresis in permalloy» *Journal of Physics D: Applied Physics* 35 , p. 2902–2908, 2002. 515
- Meng Sun, A. Balagurov «High damping in Fe-Ga-La alloys: Phenomenological model for,» *Journal of Materials Science & Technology*, vol. 72, pp. 69-80, 2021. 517
- A. Khanchehgardan, G. Rezazadeh, «Damping Ratio in Micro-Beam Resonators Based on Magneto-Thermoelasticity,» *Journal of Solid Mechanics*, vol. 9, n. 2, pp. 249-262, 2017. 519
- R. Bozorth, «Ferromagnetism,» *D. Van Nostrand Company Inc., New York*, 1951. 521
- R. Birss, «Magnetomechanical effects in the Rayleigh Region,» *IEEE Transactions on Magnetics*, MAG-7, n. 1, pp. 113-131, March 1971. 522
- M. Sablik, «A model for asymmetry in magnetic property behavior under tensile and compressive stress in steel,» *IEEE Transactions on Magnetics*, vol. 33, n. 5, September 1997. 524
- F. Beck, R.C. Gomes, «Stress dependence of the domain wall dynamics in the adiabatic regime,» *Journal of magnetism and Magnetic materials* 323 , pp. 268-271, 2010. 526
- G. Paolini, «Thermodynamic Potentials in Isotropic Elastic media with applications to Some Basic Thermoelastic problem,» *Il Nuovo Cimento*, vol. 50, pp. 409-344, August 1967. 528
- G. Paolini, «Analisi termodinamica dei Solidi Elastici Isotropi sollecitati a fatica,» *Istituto Lombardo- Accademia di Scienza e Lettere, Estratto dei rendiconti. Classe di scienze (A)*, pp. 101, 117-158, 1967. (In Italian) 530
- G. Paolini, «Thermodynamic potentials in isotropic elastic media with applications to some basic thermoelastic problems,» *Il Nuovo Cimento, Serie X*, pp. 50, 309-344, 1967. 532
- C. Zener, «Internal Friction in Solids:I,» *theory of Internal Friction in Reeds, Physical Review*, vol. 52, pp. 230-235, 1937. 534
- C. Zener, «Internal friction of Solids: II,» *General Theory of thermoelastic Internal friction. Physical review*, vol. 52, pp. 230-235, 1937. 535
- M. A. Biot, «Thermoelasticity and Irreversible Thermodynamics,» *Journal of applied physics*, pp. 240-253, 1956. 536
- D.L. Atherton, D.C. Jiles, «Effect of stress in magnetization of steel,» *IEEE Transactions on magnetics*, mag-19, n. 5, 1983. 537
- D.C. Jiles, D.L. Atherton, «Ferromagnetic Hysteresis,» *IEEE Transactions on Magnetics*, mag-19, n. 5, September 1983. 538
- M.J. Sablik, G.L. Burkhardt, H. Kwun, «A model for the effect of the low-frequency harmonic content of the magnetic induction in ferromagnetic materials» *Journal of applied Physics*, April 1988. 539
- M.J. Sablik, D.C. Jiles, «Coupled magnetoelastic theory of magnetic and Magnetostrictive hysteresis,» *IEEE Transactionson Magnetics*, vol. 29, n. 3, July 1993. 541
- M.J. Sablik, D.C. Jiles, «Modeling the effect of torsional stress on hysteretic magnetization,» *IEEE Trasnactions on Magnetics*, vol. 35, n. 1, January 1999. 543
- F.N. Tavazde, L.K. Gordienko «Internal friction in metals and alloy, Edited by V.S. Postnikov,» *Consultants Bureau, New York*, 1967. 545
- R.E.D Bishop, D. C. Johnson, «The mechanics of Vibration,» *Cambridge University Press, Cambridge*, 1979. 547
- G. Paolini, A. Lo Conte, «Smorzamento delle oscillazioni libere di un pendolo torsionale dovuto all'effetto termoelastico,» in *XXX Convegno nazionale AIAS*, Parma pp. 18-21, September 2002. (In Italian) 548